



Originally published as:

Blöschl, G., Hall, J., Parajka, J., Perdigão, R. A. P., Merz, B., Arheimer, B., Aronica, G. T., Bilibashi, A., Bonacci, O., Borga, M., Čanjevac, I., Castellarin, A., Chirico, G. B., Claps, P., Fiala, K., Frolova, N., Gorbachova, L., Gül, A., Hannaford, J., Harrigan, S., Kireeva, M., Kiss, A., Kjeldsen, T. R., Kohnová, S., Koskela, J. J., Ledvinka, O., Macdonald, N., Mavrova-Guirguinova, M., Mediero, L., Merz, R., Molnar, P., Montanari, A., Murphy, C., Osuch, M., Ovcharuk, V., Radevski, I., Rogger, M., Salinas, J. L., Sauquet, E., Šraj, M., Szolgay, J., Viglione, A., Volpi, E., Wilson, D., Zaimi, K., Živković, N. (2017): Changing climate shifts timing of European floods. - *Science*, 357, 6351, pp. 588—590.

DOI: <http://doi.org/10.1126/science.aan2506>

Title: Changing climate shifts timing of European floods

Authors:

Günter Blöschl^{1*}, Julia Hall¹, Juraj Parajka¹, Rui A. P. Perdigão¹, Bruno Merz², Berit Arheimer³, Giuseppe T. Aronica⁴, Ardian Bilibashi⁵, Ognjen Bonacci⁶, Marco Borga⁷, Ivan Čanjevac⁸, Attilio Castellarin⁹, Giovanni B. Chirico¹⁰, Pierluigi Claps¹¹, Károly Fiala¹², Natalia Frolova¹³, Liudmyla Gorbachova¹⁴, Ali Gül¹⁵, Jamie Hannaford¹⁶, Shaun Harrigan¹⁶, Maria Kireeva¹³, Andrea Kiss¹, Thomas R. Kjeldsen¹⁷, Silvia Kohnová¹⁸, Jarkko J. Koskela¹⁹, Ondrej Ledvinka²⁰, Neil Macdonald²¹, Maria Mavrova-Guirguinova²², Luis Mediero²³, Ralf Merz²⁴, Peter Molnar²⁵, Alberto Montanari⁹, Conor Murphy²⁶, Marzena Osuch²⁷, Valeryia Ovcharuk²⁸, Ivan Radevski²⁹, Magdalena Rogger¹, José L. Salinas¹, Eric Sauquet³⁰, Mojca Šraj³¹, Jan Szolgay¹⁸, Alberto Viglione¹, Elena Volpi³², Donna Wilson³³, Klodian Zaimi³⁴, and Nenad Živković³⁵

Affiliations:

¹Institute of Hydraulic Engineering and Water Resources Management, Technische Universität Wien, Vienna, Austria.

²Helmholtz Centre Potsdam, GFZ German Research Centre for Geosciences, Potsdam, Germany.

³Swedish Meteorological and Hydrological Institute, Norrköping, Sweden.

⁴Department of Engineering, University of Messina, Messina, Italy.

⁵CSE – Control Systems Engineer, Renewable Energy Systems & Technology, Tirana, Albania.

⁶Faculty of Civil Engineering, Architecture and Geodesy, Split University, Split, Croatia.

⁷Department of Land, Environment, Agriculture and Forestry, University of Padova, Padua, Italy.

⁸University of Zagreb, Faculty of Science, Department of Geography, Zagreb, Croatia.

⁹Department of Civil, Chemical, Environmental and Materials Engineering (DICAM), Università di Bologna, Bologna, Italy.

¹⁰Department of Agricultural Sciences, University of Naples Federico II, Naples, Italy.

¹¹Department Environment, Land and Infrastructure Engineering (DIATI), Politecnico di Torino, Turin, Italy.

¹²Lower Tisza District Water Directorate, Szeged, Hungary.

¹³Department of Land Hydrology, Lomonosov Moscow State University, Moscow, Russia.

¹⁴Department of Hydrological Research, Ukrainian Hydrometeorological Institute, Kiev, Ukraine.

¹⁵Department of Civil Engineering, Dokuz Eylul University, Izmir, Turkey.

¹⁶Centre for Ecology & Hydrology, Wallingford, Oxfordshire, UK.

¹⁷Department of Architecture and Civil Engineering, University of Bath, Bath, UK.

¹⁸Slovak University of Technology in Bratislava, Faculty of Civil Engineering, Department of Land and Water Resources Management, Radlinského 11, 810 05 Bratislava, Slovakia.

¹⁹Finnish Environment Institute, Helsinki, Finland.

²⁰Czech Hydrometeorological Institute, Prague, Czechia.

²¹Department of Geography and Planning & Institute of Risk and Uncertainty, University of Liverpool, Liverpool, UK.

²²University of Architecture, Civil Engineering and Geodesy, Sofia, Bulgaria.

²³Department of Civil Engineering: Hydraulic, Energy and Environment, Technical University of Madrid, Madrid, Spain.

²⁴Department for Catchment Hydrology, Helmholtz Centre for Environmental Research – UFZ, Halle, Germany.

²⁵Institute of Environmental Engineering, ETH Zurich, Zurich, Switzerland.

²⁶Irish Climate Analysis and Research Units (ICARUS), Department of Geography, Maynooth University, Ireland.

²⁷Institute of Geophysics Polish Academy of Sciences, Department of Hydrology and Hydrodynamics, Warsaw, Poland.

²⁸Hydrometeorological Institute, Odessa State Environmental University, Odessa, Ukraine.

²⁹Institute of Geography, Faculty of Natural Sciences and Mathematics, Ss. Cyril and Methodius University, Skopje, Republic of Macedonia.

³⁰Irstea, UR HHLY, Hydrology-Hydraulics Research Unit, Lyon, France.

³¹Faculty of Civil and Geodetic Engineering, University of Ljubljana, Ljubljana, Slovenia.

³²Department of Engineering, University Roma Tre, Rome, Italy.

³³Norwegian Water Resources and Energy Directorate, Oslo, Norway.

³⁴Institute of Geo-Sciences, Energy, Water and Environment (IGEWE), Polytechnic University of Tirana, Tirana, Albania.

³⁵University of Belgrade, Faculty of Geography, Belgrade, Serbia.

*Corresponding author. Email: bloeschl@hydro.tuwien.ac.at

1 **Abstract:**

2 A warming climate is expected to impact river floods; however, no consistent climate change
3 signal in observed flood magnitudes has been identified so far. ~~The seasonal timing of river~~
4 ~~floods is a sensitive signature of climate-related flood-driving processes, so any changes will~~
5 ~~shed light on climate effects on floods.~~ We have analyzed the timing of river floods in Europe
6 over the last five decades using a new pan-European database from ~~almost 5000~~ 4729
7 observational hydrometric stations. ~~We found, and find~~ clear patterns of change in flood timing.
8 Warmer temperatures have led to earlier spring snowmelt floods throughout North-Eastern
9 Europe; delayed winter storms associated with polar warming have led to later winter floods
10 around the North Sea; and some sectors of the Mediterranean Coast and earlier soil moisture
11 maxima have led to earlier winter floods in Western Europe. Our results highlight the existence
12 of a clear climate signal in flood observations at the continental scale.

13

14

15

16 **One Sentence Summary:**

17 We find that the observed timing of floods has shifted consistently in many parts of Europe over
18 the past 50 years as a result of a changing climate.

19

20 **Main Text:**

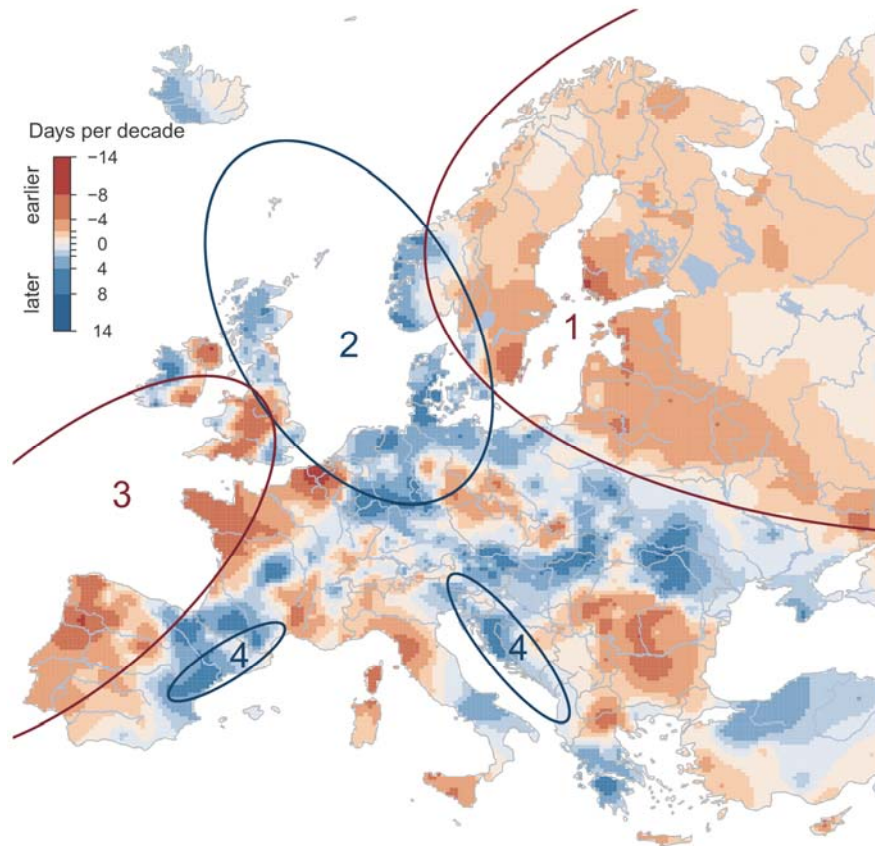
21 River flooding affects more people worldwide than any other natural hazard, with an estimated
22 global annual average loss of US \$104 billion (1). Damages are expected to increase due to
23 economic growth and climate change (2, 3). The intensification of the water cycle due to a
24 warming climate is projected to change the magnitude, frequency and timing of river floods (3).
25 However, existing studies have been unable to identify a consistent climate change signal in
26 flood magnitudes (4). Identification of a large-scale climate change signal in flood observations
27 has been hampered by the existence of many processes controlling floods, including
28 precipitation, soil moisture and snow, by non-climatic drivers of flood change such as land use
29 change and river training, and by the inconsistency of inconsistent data sets and their limited
30 spatial extents (4, 5). ~~To avoid some of these issues, it~~ has been proposed ~~to analyze that~~
31 considering the seasonal timing of floods as a fingerprint of climate effects on floods may be a
32 way to avoid some of those complications (6, 7). For example, in cold regions, earlier snowmelt
33 due to warmer temperatures leads to earlier spring floods (6), and this climate-related signal may
34 be less confounded by non-climatic drivers than flood magnitudes themselves, because of the
35 strong seasonality of climate. While the changing timing of floods has been studied at local scale
36 in Nordic and Baltic countries (8–10), no consistent analysis exists at the European scale.

37 Here we analyze ~~the most comprehensive a~~ large data set of flood observations in Europe to
38 ~~show assess whether that~~ a changing climate has shifted the timing of river floods in the last five
39 decades. Our analysis is based on river discharge or water level observations from 4947–4729
40 hydrometric stations in 38 European countries for the period 1960–2010. For each station, we use
41 a series consisting of the dates of occurrence of the highest peak in any calendar year. We
42 quantify define the average timing of the floods by the average date on which floods have
43 occurred during the observation period. We then estimate the trend in the timing of the floods

44 using the Theil-Sen's slope estimator (11) and the long-term evolution using a 10-year moving
45 average filter. Finally, we analyze the change signal of three potential drivers of flood changes in
46 a similar fashion: the ~~mid-middle~~ date of the maximum 7-day precipitation; the ~~mid-middle~~ day
47 of the month ~~of~~with the highest soil moisture; and the ~~mid-middle~~ day of the first seven days in a
48 year with air temperature above 0° C as a proxy for spring snowmelt and snowfall-to-rain
49 transition.

50 Our data show a clear shift in the timing of floods in Europe in the past 50 years (Fig. 1).
51 The regionally interpolated trend patterns shown in Fig. 1s range from a -13 days per decade
52 towards earlier floods to +9 days towards later floods (~~Fig. 1~~), which translates into total shifts of
53 -65 and +45 days, respectively, of linear trends over the entire 50 year period. The local, station
54 specific, trends (Fig. S2) are larger, but reflect smaller scale rather than regional scale processes.
55 ~~are about twice that range.~~ The changes are most consistent in North-Eastern Europe (region 1 in
56 Fig. 1) where 81% of the stations show a shift towards earlier floods (50% of the stations by
57 more than -8 days / 50 yrs). The changes are largest in Western Europe along the North Atlantic
58 Coast from Portugal to England (region 3) where 50% of the stations show a shift towards earlier
59 floods ~~of~~by at least 16 days (25% of the stations by more than 36 days). Around the North Sea
60 (region 2, South-Western Norway, the Netherlands, Denmark and Scotland) 50% of the stations
61 show a shift towards later floods by more than 7 days. In some parts of the Mediterranean Coast
62 (region 4, North-Eastern Adriatic Coast, North-Eastern Spain), there is a shift towards later
63 floods (50% of the stations by more than 6 days). Apart from the large-scale change patterns
64 described for the four regions above, smaller-scale patterns of changes in flood timing can be
65 identified. ~~Other parts of Europe exhibit smaller scale patterns.~~

66

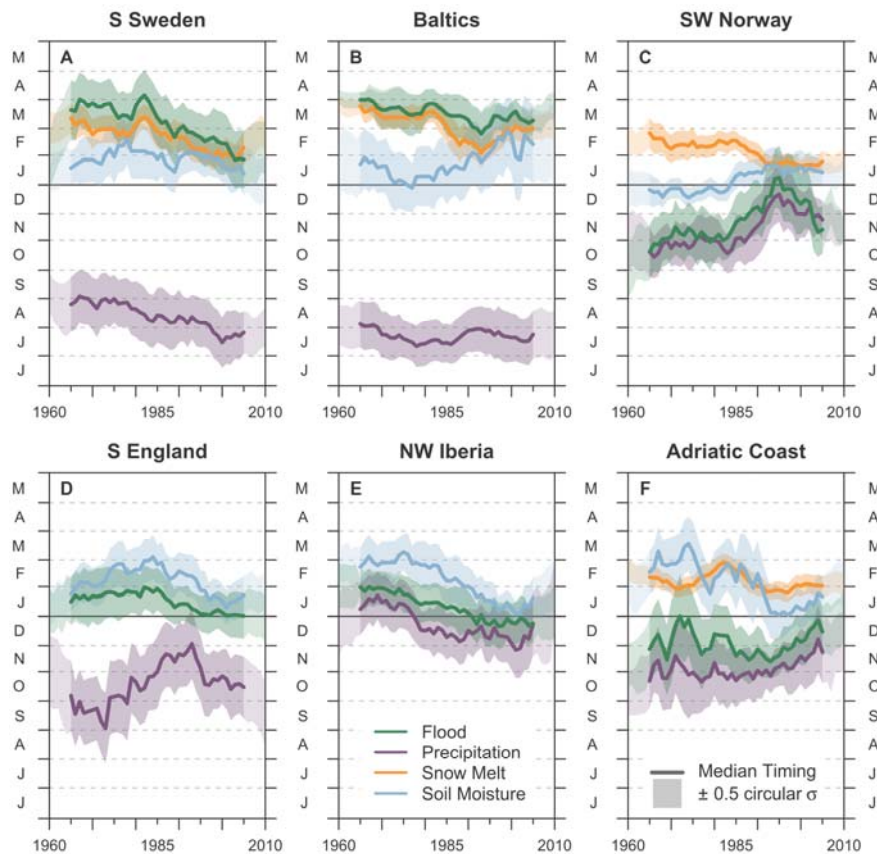


67
 68 **Fig. 1. Observed trends of river flood timing in Europe (1960-2010).** Red indicates earlier floods, blue
 69 later floods (days per decade). 1-4 indicate regions with distinct drivers. [1] North-Eastern Europe: earlier
 70 snowmelt. [2] North Sea region: later winter storms. [3] Western Europe along the Atlantic Coast: earlier
 71 soil moisture maximum. [4] parts of the Mediterranean Coast: stronger Atlantic influence in winter.
 72

73 In order to ~~interpret~~ infer the causes of these changes in timing, we focused on six sub-
 74 regions or hotspots, where changes in flood timing are particularly clear (Fig. S2, Table S2).
 75 Since floods are the result of the seasonal interplay of precipitation, soil moisture and snow
 76 processes (12) we analyzed the temporal evolutions of these variables and compared them to
 77 those of the floods (Fig. 2A-2F). In Southern Sweden (Fig. 2A) and in the Baltics (Fig. 2B),
 78 floods are mainly due to spring snowmelt (9, 10). The temporal evolution of flood timing
 79 therefore closely follows that of snowmelt, shifting from late March to February (green and

80 orange lines in Fig. 2A, 2B). Earlier snowmelt is known to be driven by both local temperature
81 increases and a decreasing frequency of [advection of arctic air masses](#) (13). The Baltics are
82 topographically less shielded [from these air masses](#) than Southern Sweden, which is reflected by
83 larger variations in the timing of snowmelt in the 1990s. In South-Western Norway (Fig. 2C)
84 precipitation maxima at the end of the year generate floods around the same time, since there is
85 little subsurface [water](#) storage capacity [there](#) due to [the prevalence of](#) shallow soils. Changes in
86 the North Atlantic Oscillation (NAO) since 1980 (14) may have resulted in a delayed arrival of
87 heavy winter precipitation, with maxima shifting from October to December. [These NAO](#)
88 [anomalies have been less pronounced since the early 2000s and which may have resulted in a](#)
89 [slight reduction of the shift in flood and precipitation timing, and a turn at the end of the series](#)
90 [back](#) to November. The floods follow [exactly closely](#) the timing of extreme precipitation
91 (Fig. 2C), which strongly suggests a causal link. The changes in the NAO may be related to Polar
92 warming, among many other factors, although the [jury is still out on the](#) role of anthropogenic
93 effects [on these still is uncertain](#) (15, 16). In Southern England (Fig. 2D), the subsurface [water](#)
94 storage capacity tends to be much larger than in coastal Norway. The maximum rainfall, which
95 occurs in autumn, therefore tends to get stored, and soil moisture and groundwater tables
96 continuously increase until they reach a maximum in winter. Sustained winter rainfall on
97 saturated soils then produces the largest floods in winter. Therefore, the flood timing in Southern
98 England is more closely associated with the timing of maximum soil moisture than with the
99 timing of extreme precipitation (17). The variations in flood timing in North-Western Iberia (Fig.
100 2E) are similar to [those of Southern](#) England, although precipitation [is there occurs](#) more [in the](#)
101 [winter dominated](#), so extreme precipitation and maximum soil moisture (driven by sustained
102 precipitation) are more closely aligned. Along the Northern Adriatic Coast (Fig. 2F), large-scale

103 Atlantic influences by the Atlantic Ocean condition Adriatic meso-scale cyclonic activity, which
 104 produces heavy precipitation towards the end of the year (18). Meridional shifts in storm tracks
 105 have increased atmospheric flow from the Atlantic to the Mediterranean in winter (19), leading
 106 to extreme precipitation and floods to peak later in the season (Fig. 2F).

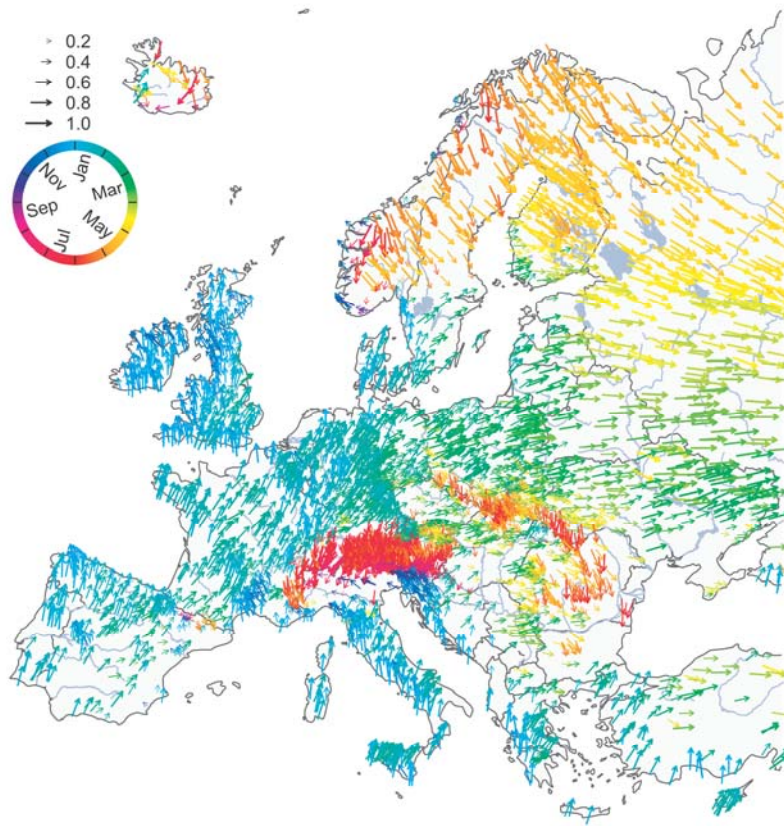


107
 108 **Fig. 2. Long-term temporal evolution of timing of floods and their drivers for six hotspots in**
 109 **Europe.** Southern Sweden (A), Baltics (B), South-Western Norway (C), Southern England (D), North-
 110 Western Iberia (E), Adriatic Coast (F). Timing of observed floods (green), 7-day maximum precipitation
 111 (purple), snowmelt indicator (orange), and timing of modeled maximum soil moisture (blue). Line shows
 112 median timing over the entire hotspot, bands indicate variability of timing within the year (± 0.5 circular
 113 standard deviation (Eq. 8). All data were subject to a 10-year moving average filter. Vertical axes show
 114 month of the year (June to May).

115

116 To further assist in the interpretation of trends in flood timing across Europe of Fig. 1, the
117 spatial pattern of the average flood timing (1960-2010) is presented in Fig. 3. The average timing
118 of the floods varies gradually from the West to the East due to increasing continentality, and
119 from the South to the North due to the increasing influence of snow processes. The effect of
120 snow storage and melt at high altitudes, e.g. in the Alps and the Carpathians (reddish arrows in
121 Fig. 3), is superimposed on this pattern. The spatial patterns of the average timing of potential
122 drivers, and their trends, are shown in Fig. S3, S4, S5.

123 Throughout North-Eastern Europe (region 1 in Fig. 1), spring occurrence of snowmelt and
124 floods (yellow and green arrows in Fig. S4A and Fig. S3) combined with a warmer climate (Fig.
125 S4A) has led to earlier floods. In the region around the North Sea (region 2 in Fig. 1), ~~winter~~
126 ~~occurrence of~~ extreme precipitation and floods in the winter (blue arrows in Fig. S3A and Fig. 3)
127 combined with a shift in the timing of extreme winter precipitation (Fig. S3B) has led to later
128 floods. In Western Europe (region 3 in Fig. 1), winter occurrence of soil moisture maxima and
129 floods (blue arrows in Fig. S5A and Fig. 3) combined with a shift in the timing of soil moisture
130 maxima (Fig. S5B) has led to earlier floods. While region 3 shows a consistent behavior in flood
131 timing changes, closely aligned with those of soil moisture, the effect of changing storm tracks
132 on precipitation are different in Southern England and North-Western Iberia, due to the opposite
133 effects of the NAO.



134
 135 **Fig. 3. Observed average timing of river floods in Europe (1960-2010).** Each arrow represents one
 136 hydrometric station (n=49474421). Color and arrow direction indicate the average timing of floods (light
 137 blue: winter floods (DJF), green to yellow: spring floods (MAM), orange to red summer floods (JJA) and
 138 purple to dark blue autumn floods (SON)). Lengths of the arrows indicate the concentration of floods
 139 within a year (R=0 evenly distributed, R=1 all floods occur on the same date).

140
 141 If the trends in flood timing continue, considerable economic and environmental
 142 consequences may arise, as society and ecosystems have adapted to the average within-within-
 143 year timing of floods. Later winter floods in catchments around the North Sea, for example, may
 144 reduce agricultural productivity due to softer ground for spring farming operations~~poorer~~
 145 ~~trafficability~~, higher soil compaction, enhanced erosion and direct crop damage (20). Spring
 146 floods occurring earlier in the season in North-Eastern Europe may limit reservoirs—the
 147 replenishment of reservoirs if managers expect later floods that never arrive, with substantial

148 reductions in water supply availability, irrigation and hydropower generation (21). Perhaps more
149 importantly, this ~~is the first~~ study ~~that~~ identifies a clear climate change signal in flood
150 observations at the continental scale using the timing of floods, which was not possible ~~so far~~
151 using flood magnitudes (4, 5, 22).

152
153

154 **References and Notes:**

- 155 1. UNISDR, “Making Development Sustainable: The Future of Disaster Risk Management.
156 Global Assessment Report on Disaster Risk Reduction” (Geneva, Switzerland: United
157 Nations International Strategy for Disaster Reduction (UNISDR), 2015).
- 158 2. H. C. Winsemius *et al.*, Global drivers of future river flood risk. *Nat. Clim. Chang.* **6**, 381–
159 385 (2016).
- 160 3. IPCC, *Managing the Risks of Extreme Events and Disasters to Advance Climate Change*
161 *Adaptation. A Special Report of Working Groups I and II of the Intergovernmental Panel*
162 *on Climate Change* (Cambridge University Press, Cambridge, UK and New York, NY,
163 USA, 2012).
- 164 4. J. Hall *et al.*, Understanding flood regime changes in Europe: a state of the art assessment.
165 *Hydrol. Earth Syst. Sc.* **18**, 2735–2772 (2014).
- 166 5. Z. Kundzewicz, *Changes in flood risk in Europe* (IAHS Press Wallingford, 2012).
- 167 6. J. Parajka *et al.*, Seasonal characteristics of flood regimes across the Alpine-Carpathian
168 range. *J. Hydrol.* **394**, 78–89 (2010).
- 169 7. R. Merz, G. Blöschl, A process typology of regional floods. *Water Resour. Res.* **39**, 1340
170 (2003).
- 171 8. D. Wilson, H. Hisdal, D. Lawrence, Has streamflow changed in the Nordic countries? –
172 Recent trends and comparisons to hydrological projections. *J. Hydrol.* **394**, 334–346
173 (2010).
- 174 9. B. Arheimer, G. Lindström, Climate impact on floods: changes in high flows in Sweden in
175 the past and the future (1911–2100). *Hydrol. Earth Syst. Sc.* **19**, 771–784 (2015).
- 176 10. D. Sarauskiene, J. Kriauciuniene, A. Reihan, M. Klavins, Flood pattern changes in the
177 rivers of the Baltic countries. *J. Environ. Eng. Landsc.* **23**, 28–38 (2015).

187

- 188 11. P. K. Sen, Estimates of the Regression Coefficient Based on Kendall's Tau. *J. Am. Stat.*
189 *Assoc.* **63**, 1379–1389 (1968).
190
- 191 12. M. Sivapalan, G. Blöschl, R. Merz, D. Gutknecht, Linking flood frequency to long-term
192 water balance: Incorporating effects of seasonality. *Water Resour. Res.* **41**, W06012 (2005).
193
- 194 13. A. Draveniece, Detecting changes in winter seasons in Latvia: the role of arctic air masses.
195 *Boreal. Environ. Res.* **14**, 89–99 (2009).
196
- 197 14. J. W. Hurrell, H. Van Loon, Decadal variations in climate associated with the North
198 Atlantic Oscillation. *Clim. Chang.* **36**, 301–326 (1997).
199
- 200 15. N. P. Gillett *et al.*, Attribution of polar warming to human influence. *Nat. Geosci.* **1**, 750–
201 754 (2008).
202
- 203 16. E. Hanna, T. E. Cropper, P. D. Jones, A. A. Scaife, R. Allan, Recent seasonal asymmetric
204 changes in the NAO (a marked summer decline and increased winter variability) and
205 associated changes in the AO and Greenland Blocking Index. *Int. J. Climatol.* **35**, 2540–
206 2554 (2015).
207
- 208 17. A. C. Bayliss, R. C. Jones, “Peaks-over-threshold flood database: Summary statistics and
209 seasonality. IH Report No. 121” (Institute of Hydrology, Wallingford, UK, 1993).
210
- 211 18. B. Ivančan-Picek, K. Horvath, N. Mahović, M. Gajić-Čapka, Forcing mechanisms of a
212 heavy precipitation event in the southeastern Adriatic area. *Nat. Hazards.* **72**, 1231–1252
213 (2014).
214
- 215 19. E. Xoplaki, J. F. Gonzalez-Rouco, J. Luterbacher, H. Wanner, Wet season Mediterranean
216 precipitation variability: influence of large-scale dynamics and trends. *Clim. Dynam.* **23**,
217 63–78 (2004).
218
- 219 20. S. Klaus, H. Kreibich, B. Merz, B. Kuhlmann, K. Schröter, Large-scale, seasonal flood risk
220 analysis for agricultural crops in Germany. *Environ. Earth Sci.* **75**, 1–13 (2016).
221
- 222 21. T. P. Barnett, J. C. Adam, D. P. Lettenmaier, Potential impacts of a warming climate on
223 water availability in snow-dominated regions. *Nature.* **438**, 303–309 (2005).
224
- 225 22. M. Mudelsee, M. Boerngen, G. Tetzlaff, U. Gruenewald, No upward trends in the
226 occurrence of extreme floods in central Europe. *Nature.* **425** (2003).
227
- 228 23. J. Hall *et al.*, A European Flood Database: facilitating comprehensive flood research
229 beyond administrative boundaries. *Proc. Int. Assoc. Hydrol. Sci.* **370**, 89–95 (2015).
230
- 231 24. J. Vogt *et al.*, “A pan-European River and Catchment Database” (2007).
232

- 233 25. M. Haylock *et al.*, A European daily high-resolution gridded data set of surface temperature
234 and precipitation for 1950-2006. *J. Geophys. Res.* **113** (2008), doi:10.1029/2008JD010201.
235
- 236 26. H. van den Dool, J. Huang, Y. Fan, Performance and analysis of the constructed analogue
237 method applied to US soil moisture over 1981-2001. *J. Geophys. Res.* **108** (2003),
238 doi:10.1029/2002JD003114.
239
- 240 27. K. V. Mardia, *Statistics of directional data* (Academic Press Inc. London, 1972).
241
- 242 28. K. V. Mardia, P. E. Jupp, in *Directional Statistics* (John Wiley & Sons, Inc., 2008;
243 <http://dx.doi.org/10.1002/9780470316979.ch6>), pp. 93–118.
244
- 245 29. H. Theil, A Rank-invariant Method of Linear and Polynomial Regression Analysis, Part 1.
246 *Proc. R. Neth. Acad. Sci.* **53**, 386–392 (1950).
247
- 248 30. P. H. Hiemstra, E. J. Pebesma, C. J. Twenhöfel, G. B. Heuvelink, Real-time automatic
249 interpolation of ambient gamma dose rates from the Dutch radioactivity monitoring
250 network. *Comput. Geosci.* **35**, 1711–1721 (2009).
251
- 252 31. D. R. Helsel, L. M. Frans, Regional Kendall Test for Trend. *Environ. Sci. Technol.* **40**,
253 4066–4073 (2006).
254
- 255 32. G. Blöschl, T. Nester, J. Komma, J. Parajka, R. Perdigão, The June 2013 flood in the Upper
256 Danube basin, and comparisons with the 2002, 1954 and 1899 floods. *Hydrol. Earth Syst.*
257 *Sc.* **17**, 5197–5212 (2013).
258
- 259 33. R Core Team: *A Language and Environment for Statistical Computing* (2016;
260 <https://www.R-project.org>).
261
- 262 34. D. Sarkar, *Lattice: Multivariate Data Visualization with R* (Springer, New York, 2008;
263 <http://lmdvr.r-forge.r-project.org>).
264
- 265 35. R. Bivand, N. Lewin-Koh, *maptools: Tools for Reading and Handling Spatial Objects*
266 (2016; <https://CRAN.R-project.org/package=maptools>).
267
- 268 36. D. Pierce, *ncdf4: Interface to Unidata netCDF (Version 4 or Earlier) Format Data Files*
269 (2015; <https://CRAN.R-project.org/package=ncdf4>).
270
- 271 37. H. Wickham, The split-apply-combine strategy for data analysis. *J. Stat. Softw.* **40**, 1–29
272 (2011).
273
- 274 38. R. J. Hijmans, *raster: Geographic Data Analysis and Modeling* (2016; [https://CRAN.R-](https://CRAN.R-project.org/package=raster)
275 [project.org/package=raster](https://CRAN.R-project.org/package=raster)).
276

- 277 39. E. Neuwirth, *RColorBrewer: ColorBrewer Palettes* (2014; [https://CRAN.R-](https://CRAN.R-project.org/package=RColorBrewer)
278 [project.org/package=RColorBrewer](https://CRAN.R-project.org/package=RColorBrewer)).
279
280 40. R. Bivand, T. Keitt, B. Rowlingson, *rgdal: Bindings for the Geospatial Data Abstraction*
281 *Library* (2016; <https://CRAN.R-project.org/package=rgdal>).
282
283 41. A. South, *rworldmap: a new R package for mapping global data. *The R Journal*. 3, 35–43*
284 *(2011)*.
285

286 **Acknowledgments:**

287 We would like to acknowledge the support of the ERC Advanced Grant “FloodChange”, Project
288 No. 291152, the Austrian Science Funds FWF as part of the Doctoral Programme on Water
289 Resource Systems (W1219-N22), the EU FP7 project SWITCH-ON (Grant No 603587) and the
290 Russian Science Foundation (Project No. 14-17-00155). The authors also acknowledge the
291 involvement in the data screening process of C. Álvaro Díaz, I. Borzi (Sicily, Italy), E.
292 Diamantini, K. Jeneiová, M. Kupfersberger, and S. Mallucci during their stays at the Vienna
293 University of Technology. We also thank L. Gaál and D. Rosbjerg for contacting Finish and
294 Danish data holders respectively and A. Christofides for pointing us to the Greek data source, B.
295 Renard (France), T. Kiss (Hungary), W. Rigott (South Tyrol, Italy), G. Lindström (Sweden) and
296 P. Burlando (Switzerland) for assistance in preparing and/or providing data or metadata from
297 their respective regions, and B. Lüthi and Y. Hundedcha for preparing supporting data to cross-
298 check the results that are not part of the paper.

299 The hydrological data used in this paper can be obtained at
300 <http://www.hydro.tuwien.ac.at/downloads/xxx>. Precipitation and temperature data is available
301 from <http://www.ecad.eu/download/ensembles/ensembles.php>. The soil moisture data can be
302 found at <http://www.esrl.noaa.gov/psd>.

303 ~~[Details on data availability and restrictions of the data used in this paper can be found in the](#)~~
304 ~~[Supplementary Material](#).~~

305 **Supplementary Materials:**

306 Materials and Methods

307 Supplementary Text

308 Figures S1 to S5

309 Tables S1 and S2

310 References (23-41)



Supplementary Materials for

Changing climate shifts timing of European floods

Günter Blöschl, Julia Hall, Juraj Parajka, Rui A. P. Perdigão, Bruno Merz, Berit Arheimer, Giuseppe T. Aronica, Ardian Bilibashi, Ognjen Bonacci, Marco Borga, Ivan Čanjevac, Attilio Castellarin, Giovanni B. Chirico, Pierluigi Claps, Károly Fiala, Natalia Frolova, Liudmyla Gorbachova, Ali Gül, Jamie Hannaford, Shaun Harrigan, Maria Kireeva, Andrea Kiss, Thomas R. Kjeldsen, Silvia Kohnová, Jarkko J. Koskela, Ondrej Ledvinka, Neil Macdonald, Maria Mavrova-Guirguinova, Luis Mediero, Ralf Merz, Peter Molnar, Alberto Montanari, Conor Murphy, Marzena Osuch, Valeryia Ovcharuk, Ivan Radevski, Magdalena Rogger, José L. Salinas, Eric Sauquet, Mojca Šraj, Jan Szolgay, Alberto Viglione, Elena Volpi, Donna Wilson, Klodian Zaimi, and Nenad Živković

correspondence to: bloeschl@hydro.tuwien.ac.at

This PDF file includes:

Materials and Methods
Supplementary Text
Figs. S1 to S5
Tables S1 to S2
References (23-41)

Materials and Methods

Data Sets

The hydrological data were obtained from a newly created European Flood Database (23) containing data ~~from 6426 hydrometric stations~~ from 38 European countries for the period 1960 to 2010. ~~Details on t~~The hydrological data ~~that used in support the findings of this study~~ was obtained from, from 64 different data are available from the data holders/sources which are listed in Table S1. The database can be obtained from <http://www.hydro.tuwien.ac.at/downloads/xxx>. ~~Licensing restrictions apply to the availability of some of this data, which can only be obtained from the original holder.~~

The downloadable database contains the date of the largest peak discharge or highest water level in each calendar year of observed record (daily mean or instantaneous discharge) for each station, ~~as well as its date of occurrence. Only the dates were analyzed here because the study focuses on the timing of floods.~~ The dates of the maximum annual floods rather than those of multiple floods within a year are analyzed for two reasons. First, the climatological average of the flood timing over a decade or a number of decades can be more meaningfully defined if only a single flood per year is considered. Second, due to data licensing issues, for some areas only the dates of annual maxima were available.

By focusing on the dates of the annual maximum floods, processes driving change can be better evaluated than by using flood magnitudes alone. Also, one can makes best use of the diverse flood data types available. As discharges and water levels are directly linked through stage-discharge relationships, the time series of the dates can be combined to increases the temporal and spatial coverage.

Stations located within the region bounded by 6.5 W - 60 E and 29.25 N - 69.25 N, with catchment areas between 5 and 100,000 km² and with more than 10 years of data during the study period were considered here. Although the data could be stratified into smaller and larger catchments, we collectively examined catchments of all areas to maintain spatial coverage and sample size. Catchments that were known-reported by the data providers to have experienced strong human modifications that could affect the timing of floods were excluded. A few stations may still be affected by human modifications, but will have little impact on the overall result since the focus is on large-scale patterns of change. To account for the uneven spatial distribution of the hydrometric stations included in the database, in areas with high station densities such as Austria, Germany, and Switzerland, only stations with at least 49 years of data in the analysis period were included. This screening resulted in a set of ~~4947~~ 4729 stations (Fig. S1A, circles) with a median catchment size of ~~354~~ 356 km². The data from these stations were used for estimating the average timing of the annual flood peaks (Fig. 3). For estimating the change in the flood timing (Fig. 1 and 2), stations with at least 35 years of data during the analysis period (70% completeness) were considered, which resulted in ~~3429~~ 3489 stations (Fig. 1B, full circles) with a median catchment size of ~~390~~ 391 km².

For each hydrometric station, the contributing catchment boundary was derived from the CCM River and Catchment Database (24) http://www.bafg.de/GRDC/EN/01_GRDC/13_dtbse/database_node.html). The river network shown in the Figures is also taken from this database. Daily gridded precipitation and mean surface temperature data from the E-OBS data set (Version 14.0) (25) for the

period 1960-2010 were used (<http://www.ecad.eu/download/ensembles/ensembles.php>). The data consist of interpolated ground-based observations from stations with spatial resolutions of $0.5^\circ \times 0.5^\circ$ and $0.25^\circ \times 0.25^\circ$. Monthly gridded soil moisture data from the CPC Soil Moisture data set (26) for the period 1960-2010 were analyzed (<http://www.esrl.noaa.gov/psd>). The data are model-calculated monthly averaged soil moisture water height equivalents with a spatial resolution of 0.5° .

Analysis Method

As a first step, we calculated for each station the average time of year ~~on-in~~ which floods have occurred during the observation period. To account for the fact that floods can occur throughout the year, all calculations were performed using circular statistics (17, 27). Only those stations for which the null hypothesis of circular uniformity (Kuiper's test (28)) was rejected (significance level, $\alpha=0.1$) were ~~retained~~used. This resulted in 4421 stations used in the analysis of the average timing and 3343 stations for the trend analysis.

Circular non-uniformity is considered necessary for a meaningful application of circular trend analysis. The date of occurrence D_i of a flood in year i was converted into an angular value θ_i by

$$\theta_i = D_i \cdot \frac{2\pi}{m_i} \quad 0 \leq \theta_i \leq 2\pi \quad (1)$$

where $D_i = 1$ corresponds to January 1 and $D_i = m_i$ to December 31, and where m_i is the number of days in that year. The average date of occurrence \bar{D} of a flood at a station is defined as (17, 27):

$$\bar{D} = \begin{cases} \tan^{-1}\left(\frac{\bar{y}}{\bar{x}}\right) \cdot \frac{\bar{m}}{2\pi} & \bar{x} > 0, \bar{y} \geq 0 \\ \tan^{-1}\left(\frac{\bar{y}}{\bar{x}}\right) \cdot \frac{\bar{m}}{2\pi} + \pi & \bar{x} \leq 0 \\ \tan^{-1}\left(\frac{\bar{y}}{\bar{x}}\right) \cdot \frac{\bar{m}}{2\pi} + 2\pi & \bar{x} > 0, \bar{y} < 0, \end{cases} \quad (2)$$

with

$$\bar{x} = \frac{1}{n} \sum_{i=1}^n \cos(\theta_i) \quad (3)$$

$$\bar{y} = \frac{1}{n} \sum_{i=1}^n \sin(\theta_i) \quad (4)$$

$$\bar{m} = \frac{1}{n} \sum_{i=1}^n m_i \quad (5)$$

where \bar{x} and \bar{y} are the cosine and sine components of the average date, respectively, \bar{m} is the average number of days per year (365.25), and n is the total number of flood peaks at that station. The concentration R of the date of occurrence around the average date is

$$R = \sqrt{\bar{x}^2 + \bar{y}^2} \quad 0 \leq R \leq 1 \quad (6)$$

which ranges from $R = 0$ (no concentration, i.e. floods are widely dispersed throughout the year) to $R = 1$ (all floods at a station occur on the same day of the year).

As a second step, we estimated the trend in the timing by the adjusted Theil-Sen's slope estimator (11, 29). This non-parametric estimator was chosen for its robustness and insensitivity to missing values and outliers. The trend estimator β is the median of the difference of dates over all possible pairs of years (i and j) within the time series,

$$\beta = \text{median} \left(\frac{D_j - D_i + k}{j - i} \right) \text{ with } k = \begin{cases} -\bar{m} & \text{if } D_j - D_i > \bar{m}/2 \\ \bar{m} & \text{if } D_j - D_i < -\bar{m}/2 \\ 0 & \text{otherwise} \end{cases} \quad (7)$$

where k makes the adjustment for the circular nature of the dates and β has units of days per year. The value of β is plotted at the respective station location in Fig. S2. To identify spatial patterns within Europe, β was spatially interpolated using the *autoKrige* function (automatic kriging) within the R *automap* package (30), which automatically fits a variogram to the spatial data. The derived trend patterns are plotted in Fig. 1 and in the background of Fig. S2.

Third, we estimated the long-term evolution in flood timing with a centered 10-year moving average filter using Equations 2-6. (with $n=10$) to reduce the short-term year-to-year variability and sharpen the focus on long-term, decadal fluctuations., but with $n=10$. We pooled these filtered series within sub-regions or hotspots that were selected based on their similarity, within a rectangular sub-region, of the average flood timing and its trends (Fig. S1). Names of the sub-regions are only indicative for a region and do not exactly correspond to any exactly defined geographic area. The series of flood timing within each hotspot were tested for evidence of a significant regionally consistent trend, using the Regional Mann-Kendall test (31). All regional trends were statistically significant at the $\alpha=0.05$ level (Table S2). For each hotspot, the median timing for each year was calculated based on the data from each station within the hotspot. A 10-year moving average filter was then applied to the annual median timing to obtain the longer-term evolution of the time series within each hotspot (solid lines in Fig. 2). Additionally, we estimated the long-term evolution of the circular standard deviation σ ,

$$\sigma = \sqrt{-2 \ln(R)} \quad (8)$$

as a measure of the spread of flood occurrence within the year across all stations in the hotspot, and plotted σ as the widths of the bands in Fig. 2.

To investigate rain-induced effects on flood timing we identified for each grid point of the E-OBS dataset the 7-day period with the maximum precipitation in any calendar year (with at least 70% of the annual data available). We assigned the midpoint of the period as the date of the 7-day maximum precipitation, and repeated all timing and change analyses analogously to the floods described above (Fig. S3). Seven days are representative of flood generation in large catchments (32). In smaller catchments, shorter rainstorms (e.g. 1 or 3 days) may be more relevant. The average timing of the 1-day and 3-day maximum precipitation in Europe based on the E-OBS data set is very similar to the average timing of the 7-day maximum precipitation (Circular Pearson correlation coefficient $r=0.91$ and $r=0.95$, respectively), therefore we consider the 7-day maximum precipitation to be also representative for smaller catchments.

To understand the effect of snow processes on the flood timing we introduced a snowmelt-timing indicator as the first full seven days in a year when surface air temperatures exceeded 0° C. We only included those grid points at which such a date could be identified meaningfully in at least 70% of the years analyzed, i.e. where the 7-day temperatures were below 0° C before they started to rise in spring. The snowmelt-timing indicator is considered a proxy for both the snowmelt season and the transition from snowfall to rainfall. Again, all timing and change analyses were repeated (Fig. S4).

When soil moisture is high, even small rainstorms may produce floods. To understand the effect of high soil moisture on floods, we identified for each grid point of the CPC Soil Moisture dataset the month of the highest soil moisture. We assigned the midpoint of the month as the date of maximum soil moisture and repeated all timing and change analyses (Fig. S5).

Only the data of grid points for which the null hypothesis of circular uniformity could be rejected ($\alpha=0.1$) were used. For clarity of the visual presentation, Fig. S3A to S5A show only every other grid point. In the hotspot analyses (Fig. 2), the maximum precipitation, snowmelt indicator and maximum soil moisture data series were first extracted based on their location within the catchment boundaries and then aggregated for each hotspot.

All the data analysis mentioned above was performed in R (33) using the supporting packages *lattice* (34), *maptools* (35), *ncdf4*(36), *plyr* (37), *raster* (38), *RColorBrewer* (39), *rgdal* (40) and *rworldmap* (41).

Supplementary Text

Author Contributions

G.B. and J.H. designed the study and wrote the first draft of the paper.

G.B. initiated the study.

J.H. collated the database with the help of most of the co-authors, and conducted the analyses.

J.P. compiled the catchment boundaries and assisted in drafting the paper.

R.P. and B.M interpreted the results in the context of underlying geophysical mechanisms.

B.A, P.M and E.S provided additional data to crosscheck the results of this study.

All authors interpreted results, and contributed to framing and revising the paper.

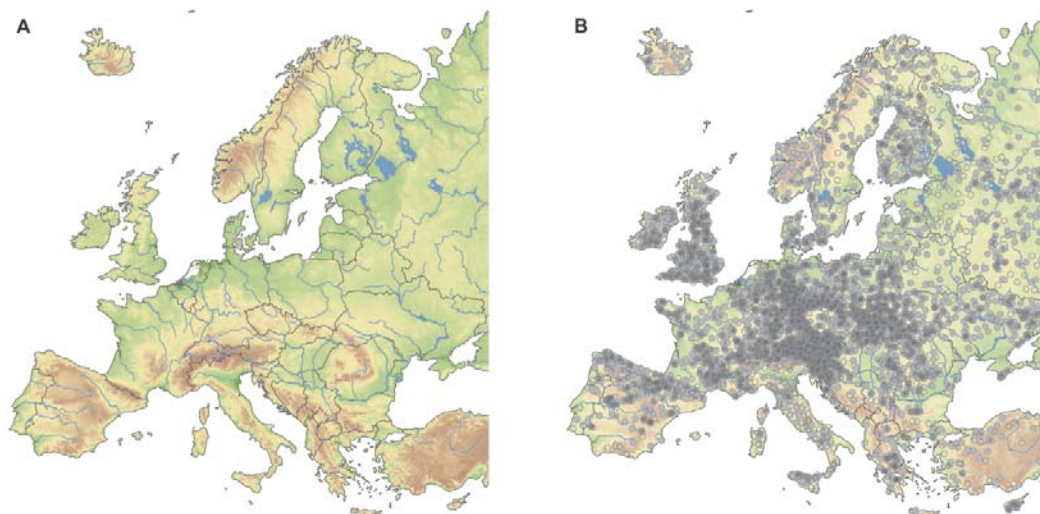


Fig. S1

Map of European study area, elevation, main rivers and lakes (**A**), and location of the hydrometric stations analyzed (**B**). Open and full circles indicate stations used for estimating the average flood timing ≥ 10 years of data, $n=49474729$), full circles indicate stations used for estimating the change in flood timing (≥ 35 years of data, $n=34293489$).

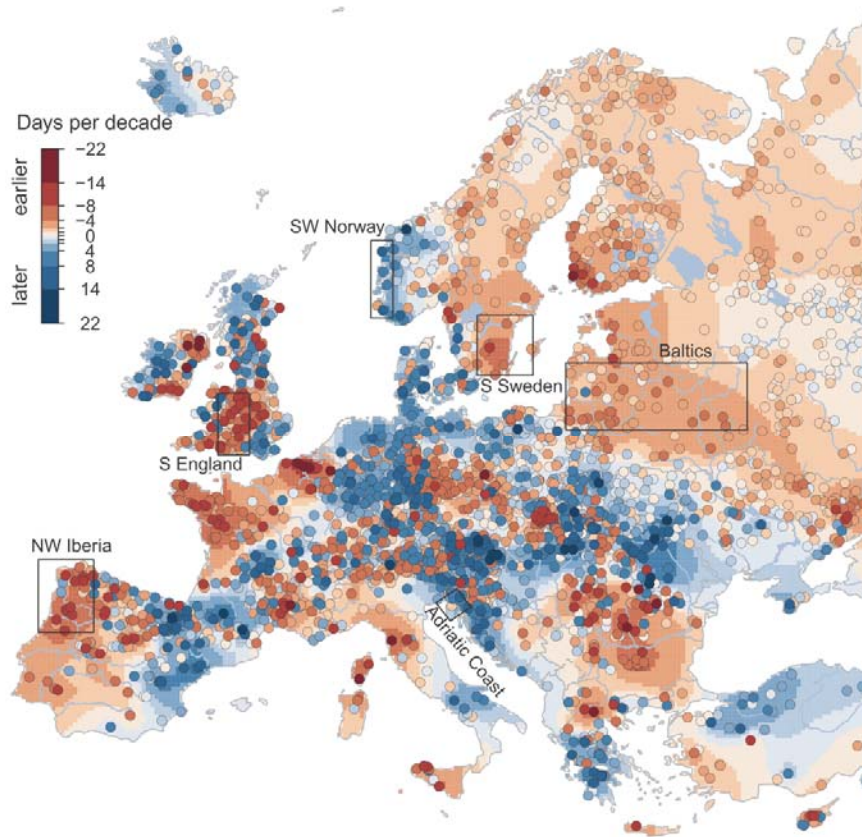


Fig. S2

Observed trends in flood timing 1960-2010, at individual hydrometric stations (points, $n=33433429$) and interpolated trends (background pattern). Rectangles show selected sub-regions that were subject to a detailed regional analysis (Fig. 2).

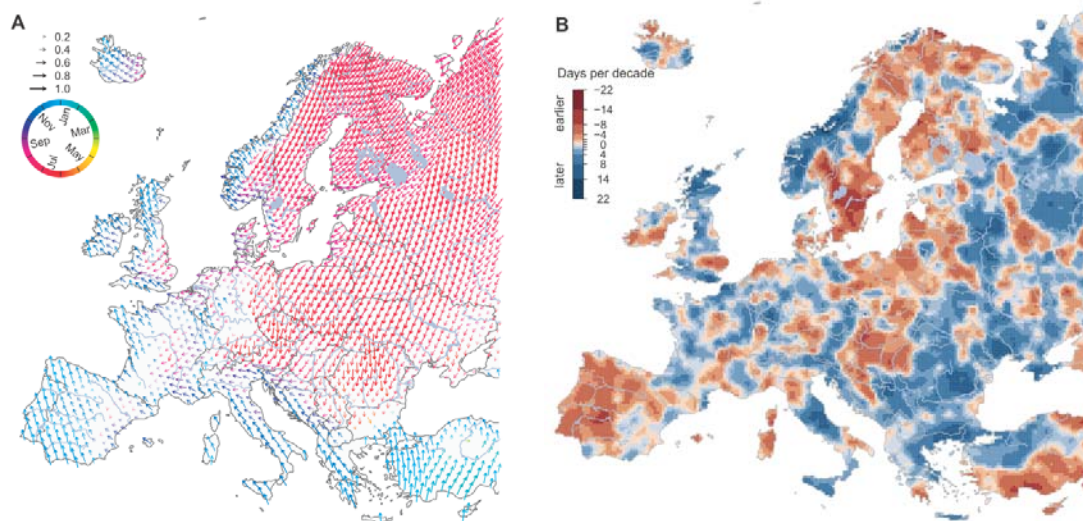


Fig. S3

7-day maximum precipitation (1960-2010). Average timing (color and direction of arrows) and concentration of timing within a year, R (length of arrows) (A), trend in timing; red indicates earlier precipitation, blue later precipitation (days per decade) (B).

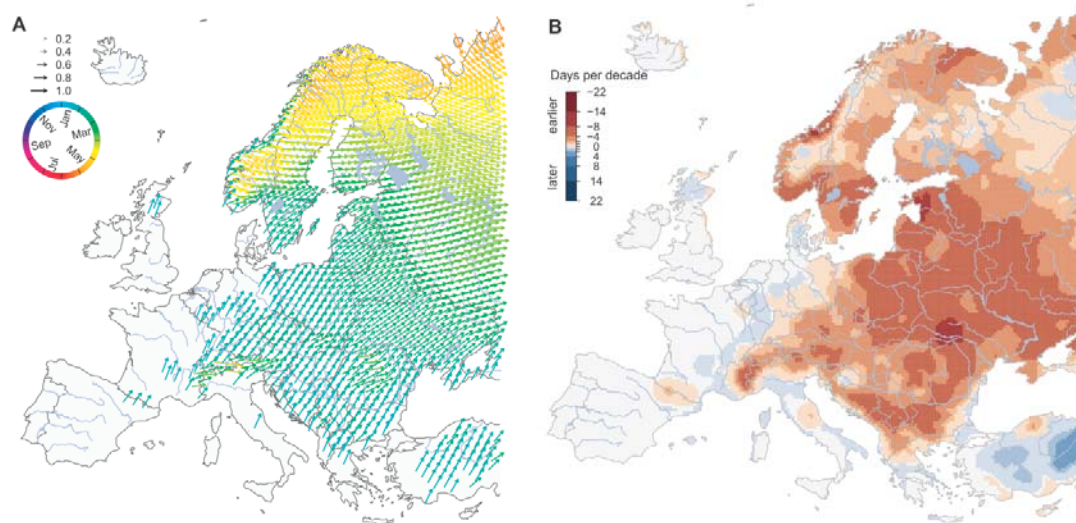


Fig. S4

Snowmelt indicator (1960-2010), first 7-days of the year with air temperature above 0° C. Average timing (color and direction of arrows) and concentration of timing within a year, R (length of arrows) (A), trend in timing; red indicates earlier snowmelt indicator, blue later snowmelt indicator (days per decade) (B).

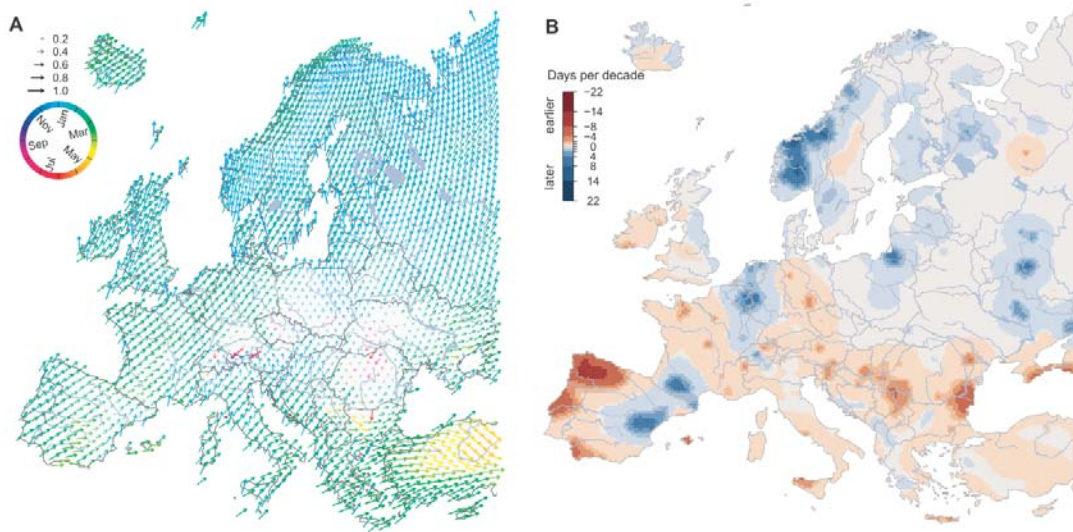


Fig. S5

Annual maximum monthly soil moisture (1960-2010). Average timing (color and direction of arrows) and concentration of timing within a year, R (length of arrows) (A), trend in timing; red indicates earlier soil moisture, blue later soil moisture (days per decade) (B).

Table S1.

Data Sources contained in the European Flood Research Database

Country/Project	Data Holder/Source/Project information
Albania	National Hydro-Meteorological Service Albania, Institute of GeoSciences, Energy, Water and Environment (IGEWE)
Austria	Hydrographic Services of Austria (HZB), Austrian Federal Ministry of Agriculture, Forestry, Environment and Water Management
Bosnia and Herzegovina	Hydrological Yearbooks of the former Republic of Yugoslavia
Bulgaria	Hydrological Yearbooks of the Rivers in Bulgaria, National Institute of Meteorology and Hydrology
Croatia	Meteorological and Hydrological Service of Croatia (DMHZ)
Czechia	Czech Hydrometeorological Institute
Denmark	Freshwater Scientific Data Centre , Danish Centre for Environment and Energy (DCE)
Estonia	Estonian Environment Agency (KAUR)
EWA	European Water Archive (EWA)
Finland	Finnish Environment Institute, Open information/Hydrology/Discharge, Source:- (SYKE)
France	HYDRO database, French Ministry of Ecology, Sustainable Development and Energy
Germany	Federal Waterways and Shipping Administration (WSV)
Germany, Bavaria	Bavarian Environment Agency (LfU)
Germany, Brandenburg	Brandenburg State Office of Environment, Health and Consumer Protection (LUGV)
Germany, Hesse	Hessian Agency for Nature Conservation, Environment and Geology (HLNUG)
Germany, Lower Saxony	Lower Saxony Water Management, Coastal Defense and Nature Conservation Agency (NLWKN)
Germany, Mecklenburg-Vorpommern	State Office of Environment, Nature Protection and Geology of Mecklenburg-Vorpommern (LUNG)
Germany, North Rhine-Westphalia	North Rhine-Westphalia State Agency for Nature, Environment and Consumer Protection (LANUV),
Germany, Rhineland-Palatinate	State Office for the Environment (LfU), Rhineland-Palatinate
Germany, Saarland	The Saarland State Office for Environmental and Labor Protection (LUA)
Germany, Saxony	Saxon State Agency for Environment, Agriculture and Geology (LfULG)
Germany, Saxony-Anhalt	State Agency for Flood Defense and Water Management of Saxony-Anhalt (LHW)
Germany, Schleswig-Holstein	Schleswig-Holstein Agency for Coastal Defense, National Park and Marine Conservation (ACNM-SH)
Germany, Thuringia	Thuringian State Institute for the Environment and Geology (TLUG)
GRDC	The Global Runoff Data Centre, Koblenz, Germany

Greece	Hydroscope- Ministry for the Environment, Energy and Climate Change - Special Secretariat for Water
Hungary	General Directorate of Water Management, Hungary
HYDRATE	HYDRATE Project data base: Hydrometeorological Data Resources and Technology for Effective Flash Flood Forecasting
Ireland	Irish Environmental Protection Agency (EPA)
Ireland	Office of Public Works (OPW)
Italy	Former National Hydrographic Service (Servizio Idrografico e Mareografico Nazionale) (SIMN)
Italy	The Italian National Institute for Environmental Protection and Research Istituto Superiore per la Protezione e la Ricerca Ambientale (ISPRA)
Italy	National Research Council—Consiglio Nazionale delle Ricerche (CNR)
Italy, <u>Bolzano</u> , South Tyrol Region	Hydrological Services, Autonomous Province of Bozen/Bolzano - South Tyrol
Italy, Emilia-Romagna Region	Regional Agency for the Environmental Protection Agenzia Regionale per la Protezione dell' Ambiente (ARPA), Emilia-Romagna
<u>Italy, Lazio & Umbria</u>	Bencivenga M., Calenda G. and Mancini C.P., 2001.
Italy, <u>Piedmont Region</u>	ENEL Italian National Agency for Electricity (Ente Nazionale per l'Energia Elettrica (ENEL))
Italy, <u>Piedmont Region</u>	IRPI (Research Institute for Hydro-Geologic Protection Istituto di Ricerca per la Protezione Idrogeologica (IRPI))
Italy, Piedmont Region	Regional Agency for the Environmental Protection (ARPA) ARPA, Piemonte
Italy, <u>Po Region</u>	Basin Authority of the Po River Autorità di Bacino del Fiume Po (AdBPo)
Italy, Sicily Region	Water Observatoy, Osservatorio delle Acque della Regione Siciliana
Italy, Trentino Region	Civil Protection Department, Autonomous Province of Trento Dipartimento Protezione Civile, Provincia Autonoma di Trento
Italy, Tuscany Region	Regional Functional Center of Meteo-Hydrological Monitoring Centro Funzionale Regionale di Monitoraggio Meteo-Idrologico, Tuscany
Italy, Veneto Region	Regional Agency for the Environmental Protection (ARPA) ARPA Veneto
Latvia	Latvian Environment, Geology and Meteorology Centre, State Ltd.
Lithuania	Lithuanian Hydrometeorological Service <u>under the Misnstry of Environment</u>
Netherlands	Rijkswaterstaat—Dutch Ministry of Infrastructure and the Environment - Rijkswaterstaat
Norway	Database Hydra II; Norwegian Water Resources and Energy Directorate Norwegian Water Resourees and Energy Directorate—Norges vassdrags-og energidirektorat (NVE)
Poland	Institute of Meteorology and Water Management National Research Institute (IMGW-PIB)

Portugal	Portuguese Environmental Agency – Agência Portuguesa do Ambiente , National Information System for Water Resources of Portugal (SNIRH)
Republic of Macedonia	National Hydrometeorological Service, Republic of Macedonia
Russia	The main hydrological characteristics, 1963–1970, 1971–75, 1975–1980, 1980–2000 Ministry of Natural Resources and Ecology of the Russian Federation; State Hydrological Institute
Russia	State Water Cadastre, 1985–2010 , State Hydrological Institute, Lomonosov Moscow State University
Russia	Automated information system of state water bodies monitoring (AIS GMVO), Russian Federal Agency for Water Resources
Serbia	Republic Hydrometeorological Service of Serbia (RHSS)
Slovakia	Slovak Hydrometeorological Institute, Bratislava (SHMI)
Slovenia	Slovenian Environment Agency (ARSO)
Spain	Centre for Hydrographic Studies (Centro de Estudios Hidrográficos) of CEDEX, Ministry of Agriculture, Food and Environment , Spain
Sweden	Swedish Meteorological and Hydrological Institute (SMHI)
Switzerland	Federal Office for the Environment (FOEN)/ (BAFU)
Turkey	General Directorate of Electrical Power Resources Survey and Development Administration (EIE), Turkey
Ukraine	Hydrological Department, Ukrainian Hydrometeorological Institute (UHMI)
Ukraine	Hydrometeorological Institute, Odessa State Environmental University (OSENUI)
United Kingdom	UK National River Flow Archive (NRFA)

Table S2.

Changes in timing for selected hotspots. Trend slopes are in days per decade. Negative signs indicate earlier flood timing, positive values later flood timing. The significance level of the regional trends is according to the Regional Mann-Kendall test.

Hotspot Name	No. of Stations	Maximum Slope	Minimum Slope	Regional Change slope	Regionally Significant
S Sweden	15	-1.58	-10.01	-5.00	$\alpha=0.01$
Baltics	43	6.52	-7.46	-3.41	$\alpha=0.01$
SW					$\alpha=0.01$
Norway	7	18.01	-2.30	9.23	
S England	53	12.34	-13.67	-4.48	$\alpha=0.01$
NW Iberia	26	2.90	-12.82	-6.87	$\alpha=0.01$
Adriatic					$\alpha=0.05$
Coast	17	9.92	-1.73	3.56	

References:

23. J. Hall *et al.*, A European Flood Database: facilitating comprehensive flood research beyond administrative boundaries. *Proc. Int. Assoc. Hydrol. Sci.* **370**, 89–95 (2015).
24. J. Vogt *et al.*, “A pan-European River and Catchment Database” (2007).
25. M. Haylock *et al.*, A European daily high-resolution gridded data set of surface temperature and precipitation for 1950-2006. *J. Geophys. Res.* **113** (2008), doi:10.1029/2008JD010201.
26. H. van den Dool, J. Huang, Y. Fan, Performance and analysis of the constructed analogue method applied to US soil moisture over 1981-2001. *J. Geophys. Res.* **108** (2003), doi:10.1029/2002JD003114.
27. K. V. Mardia, *Statistics of directional data* (Academic Press Inc. London, 1972).
28. K. V. Mardia, P. E. Jupp, in *Directional Statistics* (John Wiley & Sons, Inc., 2008; <http://dx.doi.org/10.1002/9780470316979.ch6>), pp. 93–118.
29. H. Theil, A Rank-invariant Method of Linear and Polynomial Regression Analysis, Part 1. *Proc. R. Neth. Acad. Sci.* **53**, 386–392 (1950).
30. P. H. Hiemstra, E. J. Pebesma, C. J. Twenhöfel, G. B. Heuvelink, Real-time automatic interpolation of ambient gamma dose rates from the Dutch radioactivity monitoring network. *Comput. Geosci.* **35**, 1711–1721 (2009).
31. D. R. Helsel, L. M. Frans, Regional Kendall Test for Trend. *Environ. Sci. Technol.* **40**, 4066–4073 (2006).
32. G. Blöschl, T. Nester, J. Komma, J. Parajka, R. Perdigão, The June 2013 flood in the Upper Danube basin, and comparisons with the 2002, 1954 and 1899 floods. *Hydrol. Earth Syst. Sc.* **17**, 5197–5212 (2013).
33. R Core Team: *A Language and Environment for Statistical Computing* (2016; <https://www.R-project.org>).
34. D. Sarkar, *Lattice: Multivariate Data Visualization with R* (Springer, New York, 2008; <http://lmdvr.r-forge.r-project.org>).
35. R. Bivand, N. Lewin-Koh, *maptools: Tools for Reading and Handling Spatial Objects* (2016; <https://CRAN.R-project.org/package=maptools>).
36. D. Pierce, *ncdf4: Interface to Unidata netCDF (Version 4 or Earlier) Format Data Files* (2015; <https://CRAN.R-project.org/package=ncdf4>).

37. H. Wickham, The split-apply-combine strategy for data analysis. *J. Stat. Softw.* **40**, 1–29 (2011).
38. R. J. Hijmans, *raster: Geographic Data Analysis and Modeling* (2016; <https://CRAN.R-project.org/package=raster>).
39. E. Neuwirth, *RColorBrewer: ColorBrewer Palettes* (2014; <https://CRAN.R-project.org/package=RColorBrewer>).
40. R. Bivand, T. Keitt, B. Rowlingson, *rgdal: Bindings for the Geospatial Data Abstraction Library* (2016; <https://CRAN.R-project.org/package=rgdal>).
41. A. South, rworldmap: a new R package for mapping global data. *The R Journal.* **3**, 35–43 (2011).